Available online at www.ijpe-online.com

International Journal of Performability Engineering

vol. 15, no. 12, December 2019, pp. 3262-3270
DOI: 10.23940/ijpe.19.12.p18.32623270

Analysis of the Features of Air Traffic Controllers' Eye Movements

Fei Lu[a,*], Qian Wang[a], Jingjie Teng[a], Yan Kang[b], and Bilian Liu[c]

[a]*College of Air Traffic Management, Civil Aviation University of China, Tianjin, 300300, China*
[b]*Operation Control Department, China Cargo Airlines , Shanghai, 200335, China*
[c]*Flight Department, Tianjin Air Cargo Co., Ltd., Tianjin, 300300, China*

Abstract

This paper aims to study the eye fixation and eye movements of air traffic control (ATC) controllers while working. Based on the establishment of the experimental platform of control simulation, every behavior feature of eye movement was recorded under different difficulty levels of experiments. With the geographic coordinates of the controlled area being converted to their corresponding screen coordinates, the controlled area could be divided into six zones by means of clustering analysis. The percentage of fixation points per unit in Zones 1 and 2 is dramatically greater than that of other zones, as determined by computing the fixation point per unit within the six zones. The Markov theory was applied to compute the probability of one-step fixation movement within the six zones. The results demonstrate that the highest probability of one-step fixation movement exists in Zones 1, 2, and 5, where the airspace of departure and arrival, airway crossover points, and navigation stations exist. Therefore, an experienced controller attaches a greater amount of importance and attention to the congested airspace and areas where conflict could easily occur. This paper can be used as a reference for the training of newly-employed ATC controllers to work in a safer and more efficient manner.

Keywords: air traffic controller; eye movement feature; Markov chain; fixation transfer

(Submitted on September 30, 2019; Revised on November 2, 2019; Accepted on November 12, 2019)

1. Introduction

Serving as an ATC controller requires managing an intensive workload and encountering high work risks. As such, staff must possess great responsibility and solid working skills. Since 1980, there has been a steady rise in air traffic flow of 5% per year, congesting the airspace and creating conditions of heightened workload and decreased situational awareness [1]. It is imperative to determine an effective way to improve the work ability of ATC controllers. The study of eye tracking can be traced back to psychology, and it has been applied in air traffic field research focusing on the human factors of aviation.

Stasi [2] tested the saccade feature of the ATC controller under various cognitive tasks, showing that an increased cognitive load leads to a decreased velocity of saccade, which agrees with the subjective questionnaire and operation performance of the subjects. Therefore, the velocity of saccade is sensitive to the workload of the ATC controller. The study conducted by Muller demonstrated that papillary unrest is related to cognitive load [3]. In other words, there was great papillary unrest before the cognitive load increased, which does not determine how the cognitive load was significantly increased. The study of Ahlstrom [4] on the blinking and pupil diameter of a subject revealed that the subject frequently blinked in the absence of meteorological software to control flights. Additionally, the pupil diameter of the subject was larger when working with the static-storm prediction tool, showing the increased mental load for the subject, which is in concurrence with the research results of Muller. Di [5] and his colleges found that eye-scan and fixation are related to task duration when assigned with search tasks of different difficulties, but they are unrelated to task complexity. Based on this research, Iqbal [6] put forward the concept of fixation entropy being a parameter to measure the change of work load: a signal of pre-warning was sent out when the work load increased to the safety threshold to lower or even eliminate human error.

Kang [7] classified the eye-scan modes of the ATC controller, and the eye-scan strategy was studied for aircraft conflict detection. Researchers utilized the eye tracker to evaluate how airspace complexity affects the detection of air traffic

* Corresponding author.
E-mail address: lufei315@126.com

conflict. The results demonstrated that the display of scan paths and the area of interest (AOI) can help ATC controllers solve complicated conflict detection tasks [8]. Moreover, via the eye movement experiment, it was determined that levels of ATC controllers have different identification degrees of conflict flight under mission scenarios of conflict detection with different difficulties, which can serve as a reference for the training of ATC controllers [9]. McClung [10] defined a new concept where saccade paths were classified in a simpler way, and a mapping program of visual scan path and language input was used as the theoretical basis for the analysis of the complicated saccade paths. Di [5] and others studied the effect of different work experiences on the eye movements of ATC controllers. They showed that there was no correlation between eye movement and task difficulty, although there was a link between eye movement and task duration. With the analysis of saccade sizes and average fixation time under the tasks of surveillance, plan, and control, Imants [11] found that ATC controllers used different scan modes and search strategies when assigned with tasks.

Some experiments were conducted to better understand the eye movement features of ATC controllers under the conditions of different aircraft velocity, position, and flight course into and out of control areas. The experiments were set with parameters of the number of aircrafts, the appearance time, and position. Details are presented in Table 1.

Table 1. Experimental parameters set

Task	q1	q2	q3	q4	q5
Number of aircrafts	8	10	10	12	14
Arrival aircrafts	4	6	4	7	7
Departure aircrafts	4	4	6	5	7

2. Experiment Design

2.1. Subject

In the experiment, three controllers exhibiting good physical health, normal eyesight, and the ability to complete the simulation task were used as the subjects.

2.2. Experiment Platform

The experiment platform was composed of the radar control simulator and eye tracker and functioned by the radar control simulator editor. The tasks of the radar control simulator editor were manually arranged by the number of aircrafts, the appearance time, and the airways, and they could be regarded as a real-scene model. An eye tracker of type Tobii X2-30 was utilized to record the eye movement data in the experiment.

2.3. Experiment Task

Tasks of varying difficulties in the experiment were set to order the subjects to send the flight course, velocity, and altitude instructions of air-traffic control up towards the airborne aircraft, which avoided aircraft conflicts and ensured the safety of aircraft in the airspace including the departure and arrival area.

2.4. Experiment Process

2.4.1. Experiment Preparation

Five difficulties of tasks were set before the experiment started; the aircraft sorties in the task were eight (four arrivals and four departures), ten (six arrivals and four departures), ten (four arrivals and six departures), 12 (seven arrivals and five departures), and 14 (seven arrivals and seven departures). The subjects were told the details of the experiment task at the experiment seats. The subject on the controller display, whose eye movement data was recorded by an eye tracker in tasks of different difficulties, was required to maintain his/her posture or have a slight adjustment after calibration in case of major experimental errors. The other subject was on the pilot seat to repeat the ATC instructions and obey the instructions. The experimenter needed to guarantee the power supply and normal running of the simulator and eye movement device.

2.4.2. Experiment Procedure

The experiments of different sorties were established by Latin square design.

- The eye tracker for the subject should be calibrated before the experiment is started;

- The experimenter begins the work of simultaneous recording when the subject does the job;
- After the subject completes the single task, that task will then be arbitrarily switched to another, and the experimenter records the task order;
- The experimenter records the experimental data of eye movement, and the subject leaves his/her seat when the experiment is completed.

3. Experiment Data Analysis

3.1. Traffic Control Zone Classification

The issue of incomplete data from the eye trackers may occur due to the frequent blinking and head movements of the subjects during the experiment. Additionally, the eye movement data itself will likely exhibit deviation from expected outliers. A clustering algorithm will be implemented for the data preprocessing to have a detailed zoning on the traffic area and to allow for easier analysis on the fixation feature of the subject.

The clustering points can be classified by regular density clustering to process the eye movement data, but the time sequence cannot be obtained. Therefore, the fuzzy kernel clustering algorithm should be applied as follows.

Let $x_j \in R^n (j = 1, 2, \cdots, n)$, which is the fixation points gained in the experiment. The samples are mapped by the non-continuous function Φ, and then a set of samples is obtained: $\Phi(x_1)$, $\Phi(x_2)$, $\cdots$, and $\Phi(x_n)$. $V = \{v_1, v_2, \cdots, v_t\}$ is the clustering center of the interface object, and $l = |V|$ is the number of clustering centers. $\Lambda = \{C_1, C_2, \cdots, C_t\}$ denotes the area of the interface object. u_{ij} represents x_j belonging to the membership degree of C_i and satisfies $\sum_{i=1}^{l} u_{ij} = 1$, $\forall j$, and $0 \le u_{ij} \le 1$. Finally, the target function J_m reaches the minimum and satisfies the following [12]:

$$J_m(U,V) = \sum_{i=1}^{l}\sum_{j=1}^{n} u_{ij}^{m} \left\|\Phi(x_i) - \Phi(v_i)\right\|^2, \tag{1}$$

$$\left\|\Phi(x_i) - \Phi(v_i)\right\|^2 = (\Phi(x_i) - \Phi(v_i))^T (\Phi(x_i) - \Phi(v_i)) = K(x_j, x_j) - 2K(x_j, v_i) + K(v_i.v_i) \tag{2}$$

Where $K(x, y) = \Phi(x)^T \Phi(y)$ is the kernel function, and $\left\|\Phi(x_i) - \Phi(v_i)\right\|$ defines the Euclidean distance of the feature space.

The kernel function is introduced. The inner-product operation of the feature space is transferred to kernel function computing, where the concrete form of $\Phi(x)$ does not need to be known. The Gaussian kernel function is selected.

$$K(x, y) = \exp(-\frac{\left\|x - y\right\|^2}{2\delta^2}) \tag{3}$$

Where δ is the width coefficient of the Gauss function.

Based on the theory above and according to the fixation distribution of the subject, let $k = 5$. The screen will be divided into six parts by the ATC sector boundary, with the actual airspace structure being shown in Figure 1.

Geographic coordinates are used in the airspace, whereas screen coordinates are applied in the eye movement analysis. The airport geographic coordinates should then be converted into screen coordinates. Screen coordinates are originally located in the left corner of the screen, where the positive axis of X is to the right and the positive axis of Y is downwards, which is consistent with the coordinates of the fixation point in Figure 1. The screen coordinates converted by the boundary points of controlled zones and the joint points of area classification are presented in Table 2.

3.2. Selection of the Eye Movement Parameter

The screen coordinates of fixation points converted are gained according to the principle above, and the percentage of the number of the fixation points in the unit area can be calculated. The probability of fixation transfer in and between the zones can be computed based on the Markov chain theory.

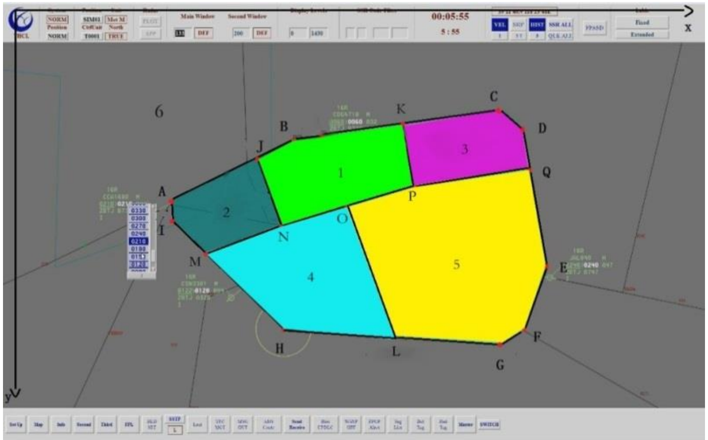

Figure 1. Screen area distribution

Table 2. Screen coordinates converted by the boundary points of controlled zones

Area joint point	Screen coordinate	Area joint point	Screen coordinate
A	(630.5823, 582.2093)	J	(802.0142, 538.236)
B	(837.9308, 529.4193)	K	(975.8094, 517.9971)
C	(1185.3712, 494.2332)	L	(1009.9174, 740.402)
D	(1224.1086, 513.0583)	M	(648.753, 616.968)
E	(1276.8382, 650.678)	N	(841.6959, 614.0337)
F	(1250.47, 721.6163)	O	(933.7906, 605.1874)
G	(1208.8138, 741.316)	P	(1012.8674, 586.6001)
H	(813.2997, 732.0351)	Q	(1248.9962, 578.1895)
I	(628.7742, 603.1877)		

3.2.1. The Percentage of the Number of Fixation Points Per Unit Area

The area of Zones 1 to 6 will be calculated accordingly, which is denoted as A after the areas are classified. The selection of the fixation points in the area will be conducted according to the eye movement data from the experiment, with the number of fixation points being gained. In the case of q2, the number of fixation points by the three subjects is exhibited in Table 4.

Table 4 shows that data deviation exists for the area that is divided in a way that is not average. Therefore, the number of fixation points per unit area should be applied as follows:

$$n_i = \frac{N_i}{A} \tag{4}$$

Where n_i is the number of fixation points per unit area in each zone, N_i is the total number of fixation points in the zones, and A is the area of the zones. p_i can then be calculated as the percentage of the fixation points per unit area.

$$p_i = \frac{n_i}{\sum_{i=1}^{6} n_i} \times 100\ \% \tag{5}$$

The percentage of the fixation points per unit area by the subject is listed in Table 5.

Table 5 shows that the percentage of fixation points per unit area in the zones significantly differs. The percentage of the fixation points in Zones 1 and 2 with less area is dramatically greater than that in other zones. This signifies that additional attention is being attached to Zones 1 and 2, where the ATC controller tends to have concentrated attention.

Table 3. The controlled area function and linear equation of controlled area boundary

Area number	Range of area joint points	Area function	Linear equation of controlled area boundary
1	JBKPONJ	Area of aircraft arrival sequence	$\begin{cases} y_{JB} = -0.255x + 742.75 \\ y_{BK} = -0.101x + 614.279 \\ y_{KP} = 1.851x - 1288.454 \\ y_{PO} = -0.235x + 824.678 \\ y_{ON} = -0.096x + 694.884 \\ y_{NJ} = 1.888x - 974.941 \end{cases}$
2	AJNMIA	Left upper airspace	$\begin{cases} y_{AJ} = -0.255x + 742.75 \\ y_{JN} = 1.888x - 974.941 \\ y_{NM} = -0.02x + 630.828 \\ y_{MI} = 0.698x + 164.138 \\ y_{IA} = -11.602x + 7898.512 \end{cases}$
3	KCDQPK	Right upper airspace	$\begin{cases} y_{KC} = -0.101x + 614.279 \\ y_{CD} = 0.486x - 81.818 \\ y_{DQ} = 2.610x - 2681.759 \\ y_{QP} = -0.036x + 622.677 \\ y_{PK} = 1.851x - 1288.454 \end{cases}$
4	MNOLHM	Left lower airspace	$\begin{cases} y_{MN} = -0.02x + 630.828 \\ y_{NO} = -0.096x + 694.884 \\ y_{OL} = 1.603x - 891.261 \\ y_{LH} = 0.023x + 712.951 \\ y_{HM} = 0.698x + 164.138 \end{cases}$
5	OPQEFGLO	Right lower airspace	$\begin{cases} y_{OP} = -0.235x + 824.678 \\ y_{PQ} = -0.036x + 622.677 \\ y_{QE} = 2.610x - 2681.759 \\ y_{EF} = -2.690x + 4085.752 \\ y_{FG} = -0.473x + 1312.978 \\ y_{GL} = 0.023x + 712.951 \\ y_{LO} = 1.603x - 891.261 \end{cases}$
6	External ATC area	Area unrelated to the task	—

Table 4. The number of fixation points by subject

Subject \ Area	1	2	3	4	5	6
Subject 1	46	107	16	51	127	944
Subject 2	74	138	27	47	82	630
Subject 3	36	60	9	55	58	324

Table 5. The percentage of the fixation point per unit area by the subject

	Area 1/%	Area 2/%	Area 3/%	Area 4/%	Area 5/%	Area 6/%
Task q1	45.74	36.03	4.44	5.89	6.89	1.01
Task q2	46.65	34.48	3.89	6.66	7.23	1.09
Task q3	45.88	34.79	4.41	6.90	6.93	1.09
Task q4	46.54	30.78	5.45	8.83	7.44	0.96
Task q5	44.99	25.25	7.83	12.67	8.15	1.11

From Tables 4 and 5, the greatest number of fixation points is found in Zone 6. However, Zone 6 also has the least number of fixation points per unit area, because Zone 6 has the biggest area with less percentage of fixation points per unit area.

3.2.2. Model of Fixation Point Transfer based on Markov Chain Theory

Markov chain theory is a way to describe the random dynamic process. If every transfer correlates with that of the previous time but has nothing to do with the past condition, this is the non-aftereffect property of Markov chain. Markov is described by the probability distribution function and makes the parameter set T as the Markov process $\{X_n, n \in T\}$, which is the discrete time set, where $T = \{0,1,2,\cdots\}$. The state space composed of all possible X_n values will be the discrete state set $I = \{i_1, i_2, i_3, \cdots\}$. Definition: let random process $\{X_n, n \in T\}$, and for any integer $n \in T$ and any $i_0, i_1, i_2, \cdots, i_{n+1} \in I$, the conditional probability will satisfy

$$P\{X_{n+1} = i_{n+1} \mid X_0 = i_0, X_1 = i_1, X_n = i_n\} = P\{X_{n+1} = i_{n+1} \mid X_n = i_n\} \tag{6}$$

Where $\{X_n, n \in T\}$ is the Markov chain [13].

The probability distribution function $P\{X_{m+1} = j \mid X_m = i\}$ refers to the probability of condition *j* at time *m*+1 when the system is under condition *i* at time *m*. This is the one-step transfer probability of the Markov chain.

The research conducted by Endsley [14] shows that the processing of information by man is first made by recognition, then by understanding, and, finally, to prediction. The different ways of data process exerted on the eye movement will be the transfer way of fixation. According to the transfer feature of fixation by each subject, Markov chain theory will be applied in the analysis of the one-step transfer probability of fixation by the subject.

Let *i* refer to the interest area where the fixation points are at the time *n*, and the conditional probability $P\{X_{m+1} = j \mid X_m = i\}$ (one-step transfer to interest area *j*). The one-step transfer probability correlates with the departure of interest area *i* and the arrival of interest area *j*, and it has nothing to do with the time *m*. The one-step transfer probability of fixation by the subject can then be calculated. When the fixation points fall at the area *i*, a_{ij} is the frequency of fixation from Zone *i* to Zone *j*, a_i is the sum of the frequency of fixation from Zone *i* to other zones, $a_i = \sum_{j=1}^{n} a_{ij}$, and *n* is the number of all interest areas. The one-step transfer probability of fixation from Zone *i* to Zone *j* will be

$$p_{ij} = \frac{a_{ij}}{a_i} \tag{7}$$

Zone 6 is a non-controlled area, and it can be understood from Table 3 that the percentage of the number of fixation points and the fixation time per unit area in Zone 6 is only 1%. The data is exhibited in Table 6.

Table 6. Distribution mean

Task	The total number of transfer in Zones 1-5	The total number of transfers in Zone 6	The total transfer number
q1	151.50	794.00	945.50
q2	181.93	819.40	1001.33
q3	138.50	546.50	685.00
q4	186.45	831.30	1017.75
q5	236.00	894.20	1130.20

All the transfer probabilities of fixation related to Zone 6 will not be taken into account, as Zone 6 is not the controlled area, the fixation points are ineffective, the number of transfers in Zone 6 is significantly greater than that of other zones, and the fixation time per unit area in Zone 6 is only 1%. Therefore, the transfer probability of fixation is only studied in Zones 1 to 5. The transfer probability of fixation by subject under tasks q1 to q5 is listed in Figures 2 to 6.

As can be observed from Figures 2 to 6, the probability of interactive transfer between Zones, 1, 2, and 5 is noticeably greater than that of other zones under all tasks, and the average transfer probability of fixation in the three zones is greater than 30%. It can be concluded that a greater percentage and probability of the number of fixation points in Zones 1 and 2 will be achieved by the subject.

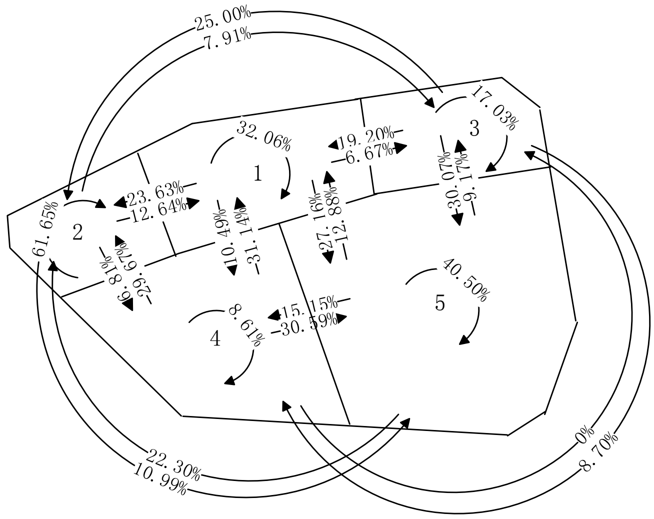

Figure 2. One-step transfer probability of fixation at all zones in task 1

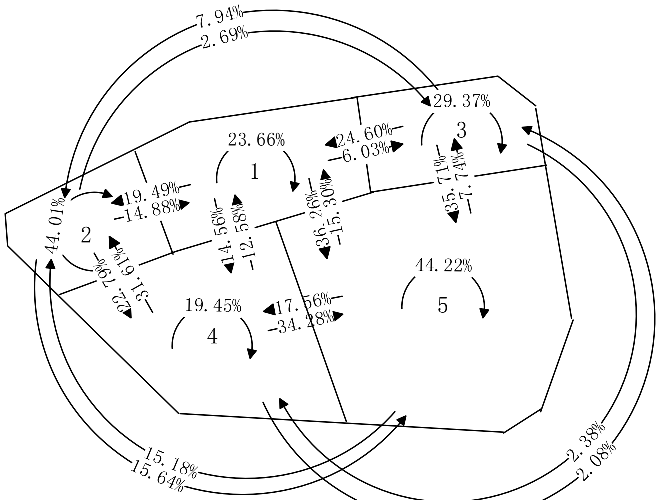

Figure 3. One-step transfer probability of fixation at all zones in task 2

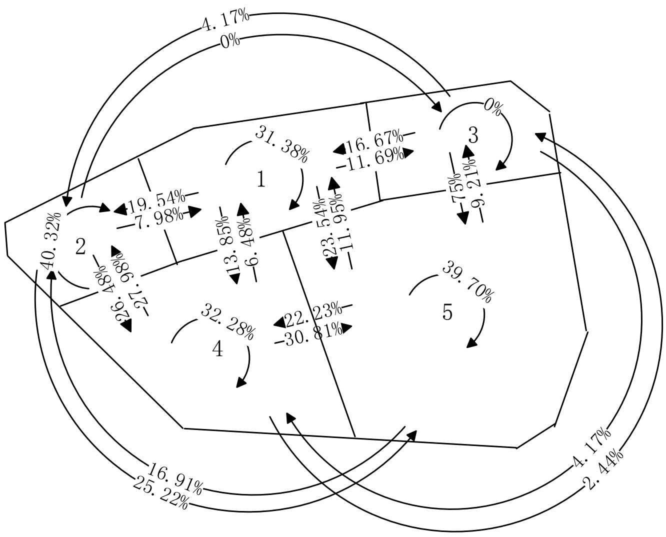

Figure 4. One-step transfer probability of fixation at all zones in task 3

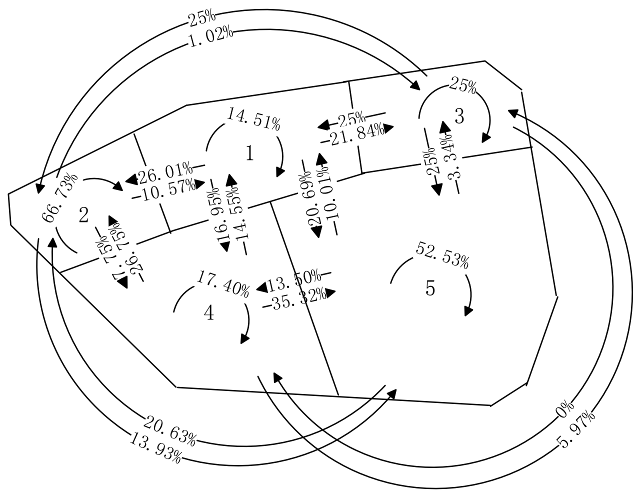

Figure 5. One-step transfer probability of fixation at all zones in task 4

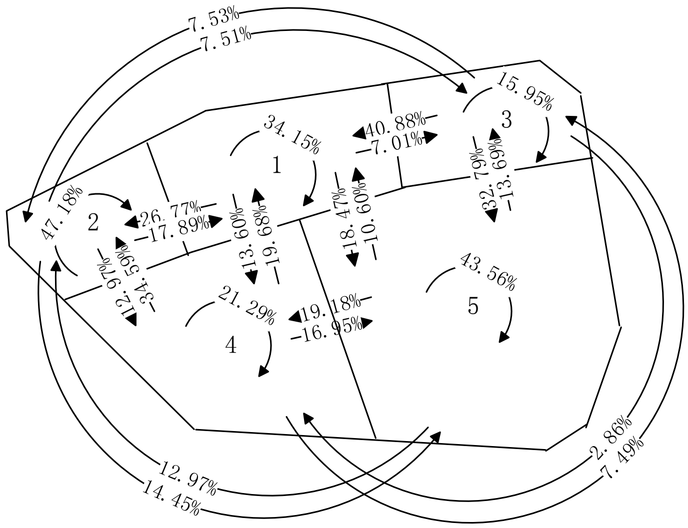

Figure 6. One-step transfer probability of fixation at all zones in task 5

For the controlled tasks arranged, Zone 1 includes the aircraft departure and arrival, Zone 2 includes the converge points of four airways, and Zone 5 includes two navigation stations, whereas there are no important marks or joint points related to flights in Zones 3 and 4. An experienced ATC controller has a greater likelihood of focusing on the busy airspace and areas where conflict easily occurs. This result can provide a good reference for newly-employed ATC controllers to work in a safer and more efficient manner.

4. Conclusions

More fixation points are in Zone 6 due to it encompassing a larger area, not necessarily its importance. These factors contribute to the smaller number of fixation points per unit area, though a significant number of points occur in Zone 6. A greater percentage of fixation points per unit area by subject occurs in Zones 1 and 2.

By implementing Markov chain theory, the highest probability of one-step transfer occurs in Zones 1, 2, and 5, where the departure and arrival area, airway converge points, and navigation stations are included, demonstrating the fact that experienced ATC controllers preferred to give more attention to the congested airspace and areas where conflict easily occurs.

The experiment results could provide a valuable reference for the training of newly-employed ATC controllers to work in a safer and more efficient manner.

Acknowledgements

The authors were supported by the National Natural Science Foundation of China (No. 71701202) and Fundamental Research Funds for the Central Universities (No. 3122014D037).

References

1. P. V. Paubel, P. Averty, and E. Raufaste, “Effects of an Automated Conflict Solver on the Visual Activity of Air Traffic Controllers,” *International Journal of Aviation Psychology*, Vol. 23, No. 2, pp. 181-196, 2013
2. L. L. D. Stasi, M. Marchitto, A. Antolí, T. Baccino, and J. J. Canas, “Approximation of on-Line Mental Workload Index in ATC Simulated Multitasks,” *Journal of Air Transport Management*, Vol. 16, No. 6, pp. 330-333, 2010
3. A. Müller, R. Petru, L. Seitz, I. Englmann, and P. Angerer, “The Relation of Cognitive Load and Pupillary Unrest,” *International Archives of Occupational and Environmental Health*, Vol. 84, No. 5, pp. 561, 2011
4. U. Ahlstrom and F. J. Friedmanberg, “Using Eye Movement Activity as a Correlate of Cognitive Workload,” *International Journal of Industrial Ergonomics*, Vol. 36, No. 7, pp. 623-636, 2006
5. S. L. Di, M. B. Mccamy, A. Catena, S. L. Macknik, J. J. Canas, and S. M. Conde, “Microsaccade and Drift Dynamics Reflect Mental Fatigue,” *European Journal of Neuroscience*, Vol. 38, No. 3, pp. 2389-2398, 2013
6. M. U. Iqbal, B. Srinivasan, and R. Srinivasan, “Towards Obviating Human Errors in Real-Time Through Eye Tracking,” *Computer Aided Chemical Engineering*, Vol. 43, pp. 1189-1194, 2018
7. Z. Kang, E. J. Bass, and D. W. Lee, “Air Traffic Controllers' Visual Scanning, Aircraft Selection, and Comparison Strategies in Support of Conflict Detection,” *Journal of Tropical Pediatrics*, Vol. 58, No. 1, pp. 77-81, 2014
8. M. Marchitto, S. Benedetto, T. Baccino, and J. J. Canas, “Air Traffic Control: Ocular Metrics Reflect Cognitive Complexity,” *International Journal of Industrial Ergonomics*, Vol. 54, pp. 120-130, 2016
9. Z. Kang and S. J. Landry, “An Eye Movement Analysis Algorithm for a Multielement Target Tracking Task: Maximum Transition-based Agglomerative Hierarchical Clustering,” *IEEE Transactions on Human-Machine Systems*, Vol. 45, No. 1, pp. 13-24, 2015
10. S. N. Mcclung and Z. Kang, “Characterization of Visual Scanning Patterns in Air Traffic Control,” Hindawi Publishing Corp. 2016
11. P. Imants and T. D. Greef, “Using Eye Tracker Data in Air Traffic Control,” in *Proceedings of the 29th Annual European Conference on Cognitive Ergonomics*, pp. 259-260, Rostock, Germany, 2011
12. S. C. Chen and X. Y. Wu, “Online Kernel Fuzzy C-Means Clustering Algorithm,” *Systems Engineering and Electronics*, Vol. 34, No. 12, pp. 2599-2606, 2012
13. C. H. Liu, “Stochastic Process (Fifth edition),” Huazhong University of Science & Technology Press, Wuhan, 2014
14. M. R. Endsley, “Toward a Theory of Situation Awareness in Dynamic Systems,” *Human Factors*: *The Journal of the Human Factors and Ergonomics Society*, Vol. 37, No. 1, pp. 32-64, 1995